Title
Method for Accurate Determination of the Electron Contribution: Specific Heat of Ba0.59K0.41Fe2As2

Authors
Rotundu, Costel R
Forrest, Thomas R
Phillips, Norman E
et al.

Publication Date
2017

DOI
10.1007/978-3-319-52675-1_23

Peer reviewed

Chapter 23
Method for Accurate Determination of the Electron Contribution: Specific Heat of $Ba_{0.59}K_{0.41}Fe_2As_2$

Costel R. Rotundu, Thomas R. Forrest, Norman E. Phillips, and Robert J. Birgeneau

Introduction

The 1986 discovery of superconductivity in $La_{1.85}Ba_{0.15}CuO_4$ (LBCO) at a critical temperature T_c of 35 K by Bednorz and Müller [1] was a milestone in the search for superconductivity in materials with higher T_c, and an important contribution to the

Costel R. Rotundu and Thomas R. Forrest contributed equally to this work.

C.R. Rotundu
Materials Sciences Division, Lawrence Berkeley National Laboratory, Berkeley, CA, 94720, USA

Stanford Institute for Materials and Energy Sciences, SLAC National Accelerator Laboratory, 2575 Sand Hill Road, Menlo Park, CA, 94025, USA

T.R. Forrest
Department of Physics, University of California, Berkeley, CA, 94720, USA

Diamond Light Source, Harwell Science and Innovation Campus, Didcot, Oxfordshire, OX11 0DE, UK

N.E. Phillips (✉)
Materials Sciences Division, Lawrence Berkeley National Laboratory, Berkeley, CA, 94720, USA

Department of Chemistry, University of California, Berkeley, CA, 94720, USA
e-mail: nephill@berkeley.edu

R.J. Birgeneau
Materials Sciences Division, Lawrence Berkeley National Laboratory, Berkeley, CA, 94720, USA

Department of Physics, University of California, Berkeley, CA, 94720, USA

Department of Materials Science and Engineering, University of California, Berkeley, CA, 94720, USA

A. Bussmann-Holder et al. (eds.), *High-Tc Copper Oxide Superconductors and Related Novel Materials*, Springer Series in Materials Science 255,
DOI 10.1007/978-3-319-52675-1_23

incentive for further research in this area. Soon after the discovery of LBCO, cuprates with much higher T_c's were found. Other classes of superconductors, some of which are remarkable include MgB_2 [2] with its highest T_c among BCS superconductors and the iron pnictide high temperature superconductors [3]; they were discovered in 2001 and 2008, respectively.

These high-T_c superconductors make an important contribution to the understanding of superconductivity, but they pose a new challenge to the determination of the conduction-electron contribution to the specific heat, a useful source of the values of important parameters and other information relevant to the nature of the superconductivity. In the conventional analyses of specific-heat data the electron contribution (C_e), (C_{es}) in the superconducting state and (C_{en}) in the normal state, is obtained by subtracting the contribution of the lattice vibrations (C_{lat}) from the total measured specific heat (C), and therein lies the problem: High values of T_c ensure high values of the upper critical field (H_{c2}) effectively eliminating the normal-state specific-heat measurements that give C_{lat} by analyzing the normal-state C as the sum of C_{lat} and $C_{en} = \gamma_n T$. As a consequence, C_{lat} has to be obtained by some kind of approximation, and the requirements are stringent: Meaningful analysis and interpretation of the resulting C_{es} requires that the approximation for C_{lat} be valid over a wide range of temperature for $T \leq T_c$. The fact that many different approximations have been used attests the general recognition of the difficulty of the problem. The approximations used include fitting normal-state data above T_c to obtain C_{lat} and extrapolating the result to low T, and using C_{lat} for a structurally similar non-superconducting material. The problem is compounded by the fact that for these materials C_{es} is a small fraction of C_{lat} at the temperatures of interest for determining the order parameter in the superconducting state, and the errors in C_{lat} are greatly magnified in C_{es}. The analysis of the C data should give the conduction-electron density of states (DOS) and the values of the energy gaps in the superconducting state, but the conventional analyses gives a variety of results for these parameters in similar materials that reflect the errors in the approximations for C_{lat}. Recently we recognized that the α model, which gives a good representation of C_{es}, offers a way out of this dilemma: We showed that C_{es} for $Ba_{0.59}K_{0.41}Fe_2As_2$ could be extracted directly from the total C data by using α-model expressions for C_{es}, bypassing the need for an independent determination of C_{lat} [4]. That paper included discussions of C_{lat}, its proper mathematical representations in different temperature regions, the approximations used in the conventional analyses, and a comparison of our results for $Ba_{0.59}K_{0.41}Fe_2As_2$ with those obtained by conventional analyses of specific-heat data on similar materials as well as with results obtained by ARPES. Here we offer a reorganized and somewhat simplified description of the basic analytical procedures, without the supporting material.

Contributions to the Specific Heat; The Determination of the Lattice Contribution

The normal-state electron contribution to C is usually taken to be

$$C_{en} \equiv \gamma_n T, \tag{23.1}$$

where γ_n is a temperature-independent constant (but see below) that is proportional to the DOS. If there are two bands γ_n represents the sum of the two contributions. (When it is convenient to distinguish the specific-heat contributions or other properties of two bands, additional subscripts, 1 and 2, are used, e.g., $\gamma_n = \gamma_{n1} + \gamma_{n2}$, $C_{es} = C_{es1} + C_{es2}$, α_1 and α_2, etc.)

The superconducting-state electron contribution given by the BCS theory in the weak-coupling limit, has been tabulated by Mühlschlegel [5] in the form $C_{es}/\gamma_n T_c$ as a function of the reduced temperature, $t \equiv T/T_c$. Experimental results for strong-coupling materials are inconsistent with this result, and they are also inconsistent with general limitations on the effects of strong coupling in the BCS theory [6]. This led to the formulation of the α model [6], a phenomenological extension of the BCS theory to include strong-coupling effects. In the α model the temperature dependence of the energy gap is taken to be that calculated [5] for the BCS theory in the weak-coupling limit, but the amplitude of the gap at $T = 0$, $\Delta(0)$, is an adjustable parameter represented by $\alpha \equiv \Delta(0)/k_B T_c$ that provides an empirical measure of the strength of the coupling. In the weak-coupling limit of the BCS theory $\alpha = 1.764 \equiv \alpha_{BCS}$. Early applications were focused on superconductors that showed other evidence of strong coupling, which gave values of α greater than α_{BCS}, but for some superconductors the thermodynamic properties were represented by values of α less than α_{BCS}, and recently this has been interpreted in terms of weak coupling. For MgB_2 at the lowest temperatures C_{es} shows a large excess over that given by the BCS theory. It was recognized [7] that this could be represented by the α model with α *much* less than α_{BCS}, but this would not be consistent with C_{es} near T_c (see Fig. 2 of [7]). This suggested the extension of the α model to a two-band, two-gap superconductor in which C_e is taken to be the sum of two independent additive contributions, even though the equality of T_c in the two bands requires some interband coupling [7]. The α-model fits represent C_{es} for MgB_2 to within the experimental accuracy [7] giving α values of 2.2 and 0.6, which are consistent with detailed theoretical calculations [8] that show both strong and weak coupling. Currently, essentially all specific heat measurements on high-T_c Fe pnictide superconductors are compared with a model of this kind.

The vortex-state electron contribution of a superconductor with an isotropic gap includes two terms:

$$C_{ev}(H) = C_{evs}(H) + \gamma_v(H)T. \tag{23.2}$$

The first term, $C_{evs}(H)$, which is associated with the residual superconducting condensate, is the in-field counterpart of C_{es} in zero field. It decreases in magnitude

with increasing H but the details of its H and T dependences are not theoretically established. The other term, $\gamma_v(H)T$, is associated with localized quasiparticle states in the vortex cores [9]. Its coefficient varies from $\gamma_v(0) = 0$ to $\gamma_v(H_{c2}) = \gamma_n$, with a variation that is, at least for a single-band superconductor, linear in H. (Non-linear variations associated with structure in the energy gaps are considered in section "Discussion".) In most samples of superconducting materials there is a "residual" DOS that produces a normal-state-like contribution to C even in zero field. This appears as a non-zero value of $\gamma_v(0)$, $\gamma_r \equiv \gamma_v(0) \neq 0$, and is generally attributed to non-superconducting regions of the same material.

It is generally accepted that in the low-T limit the lattice contribution can be represented by

$$C_{lat} = \mathrm{B}_3 T^3 + \mathrm{B}_5 T^5 + \mathrm{B}_7 T^7 + \quad , \tag{23.3}$$

with

$$\mathrm{B}_3 = (12/5)\pi^4 \mathrm{R}/{\theta_\mathrm{D}}^3, \tag{23.4}$$

where θ_D is the Debye temperature. The higher-order terms represent the effects of phonon dispersion, and they may also serve as an approximation for the low-T contributions of low-frequency optical modes if the lattice has a basis with more than one atom in the primitive unit cell. However, Eq. (23.3) is often used in an interval of temperature at higher temperatures, in which case it is just a convenient fitting expression with no physical meaning. In particular, coefficients obtained in the high-T fits cannot be expected to give a valid expression for C_{lat} at lower temperatures. Combinations of Debye and Einstein functions are also used to represent C_{lat} at higher temperatures, where they are physically more reasonable fitting expressions, but the fits are relatively insensitive to the values of the fitting parameters, and the parameters derived, like those derived from high-T fits with Eq. (23.3), should not be expected to give C_{lat} accurately at lower temperatures.

For the high-T_c Fe pnictides two methods for obtaining an approximation for C_{lat} for $T \leq T_c$ have been used. In one, the first step is to obtain C_{lat} for $T \leq T_c$ for a comparison material for which the normal-state specific heat is known. The comparison materials that have been used include the undoped non-superconducting parent compound, an overdoped non-superconducting sample, and a material with a different dopant that suppresses both the superconductivity and the high-T structural/magnetic transition. In some cases adjustments to C_{lat} of the comparison material for the differences in stoichiometry or structure are made, but they are necessarily rough approximations. Furthermore, the effect on C_{lat} of the substantial differences in the DOS are quite generally ignored. The other method is to obtain C_{lat} for the sample itself by fitting the normal-state data for $T \geq T_c$ with $C = \gamma_n T + C_{lat}$, and extrapolating the resulting C_{lat} to $T < T_c$. In addition to the fact that an expression obtained for C_{lat} in a high-T interval cannot be expected to be accurate at low temperatures, there are other reasons for doubting the validity of the derived C_{lat} (and also γ_n, if it is derived in the fit): Since C is measured at

constant pressure it includes a contribution to C_{lat} associated with the anharmonicity of the lattice vibrations that can also be approximately T proportional [10]. For samples of $Ba_{1-x}K_xFe_2As_2$ this contribution has been estimated [11] to increase rapidly from zero at $T = 0$ to ~600 mJ K^{-1} mol^{-1} at 100 K, to increase less rapidly at higher temperatures, and to become more nearly T proportional above 150 K, with a coefficient ~ 12 mJ K^{-2} mol^{-1}. Furthermore, the phonon enhancement that contributes to γ_n, and therefore γ_n itself, is expected to be T dependent (see, e.g., [12, 13]). The complicated temperature dependence of C_{lat}, including the anharmonic contribution, prevents the identification of this effect in specific-heat measurements, but there is compelling evidence for its reality in cyclotron resonance experiments [14]. There is no basis for estimating its magnitude in the Fe pnictides, but it could be substantial. The difficulties associated with obtaining an independent approximation for C_{lat}, ensure substantial uncertainty in any C_{es} obtained in the conventional analyses.

The determination of C_{lat} is the major obstacle to obtaining C_e from experimental data, but in most samples there are paramagnetic centers that also make a significant contribution to C, which is best represented by an H-dependent approximation to a Schottky function, $C_{\mathrm{Sch}}(H)$. With this contribution, the total specific heat in a field H is

$$C(H) = C_{lat} + C_e(H) + \mathrm{m}C_{\mathrm{Sch}}(H), \tag{23.5}$$

where m is the molar concentration of paramagnetic centers. For $0 \leq H < H_{c1}$, where H_{c1} is the lower critical field (and omitting the possible $\gamma_r T$ contribution) $C_e(H) = C_{es}$; for $H_{c1} \leq H < H_{c2}$, $C_e(H) = C_{evs}(H) + \gamma_v(H)T$; for $H \geq H_{c2}$, $C_e(H) = \gamma_n T$.

The requirement of entropy conservation, the equality of the conduction-electron entropies in the normal and superconducting states at T_c, is frequently invoked, either as a constraint in a fitting procedure used to obtain C_{lat} or as a test of the validity of a derived C_{lat}. In zero field it takes the form

$$\int (C_{es}/T)dT = \gamma_n T_c, \tag{23.6}$$

where $C_{es} = C - C_{lat}, -\mathrm{m}C_{\mathrm{Sch}}$ and the integration extends from $T = 0$ to $T = T_c$. In the special case of a C_{lat} that is determined in a high-temperature fit to normal-state data and then extrapolated to low temperatures, imposition of the entropy-conservation constraint can reduce gross errors in the derived C_{lat} (a detailed analysis is presented in Sect. 6 of [4]). More generally however, its effect is limited by the small fraction of the entropy at T_c that is electron entropy, e.g., ~13% in the results reported here. At best, even if an accurate value of γ_n is known independently, satisfaction of Eq. (23.6) shows only that C_{es} gives the correct *entropy* at T_c, i.e., that it is only a T^{-1}-weighted *average* of C_{es} that is correct. This leaves room for T-dependent errors that are comparable in magnitude to small contributions to C_{es} that have been attributed to small-gap bands in temperature intervals near or

below $T_c/2$. An incorrect value of γ_n will tend to produce values of C_{es} that are, on the average, either too high or too low. Furthermore, in many cases the validity of the value of γ_n used in Eq. (23.6) is not obvious, and in some cases its origin is not specified.

Samples and Measurements

Nearly optimally doped $Ba_{0.59}K_{0.41}Fe_2As_2$ single crystals were grown by a self-flux method [15]. The potassium doping value reported is as determined by inductively coupled plasma and its homogeneity is confirmed by electron microprobe wavelength-dispersive X-ray spectroscopy. The superconducting transition with an onset of 36.9 K has a width of ~1 K, as measured by magnetization. It is well known that magnetization measurement cannot provide a reliable value of the volume fraction of superconductivity. Instead, the residual DOS in the superconducting state, which is measured by the value of γ_r, is the best measure of the volume fraction of superconductivity. For our sample $\gamma_r = 0$ (see section "Specific-Heat Results and Analysis") suggesting 100% superconductivity. This is in agreement with the absence of a heat capacity signature near 70 K that would indicate the presence of FeAs, a common impurity reported in the series (see, e.g., [2, 11]). The sharp step-like magnetization at T_c, the absence of a residual DOS in the superconducting state, the absence of a detectable level of FeAs, the low concentration of paramagnetic centers (see section "Specific-Heat Results and Analysis"), and the discontinuities in C_e and its temperature derivative at T_c (see section "Specific-Heat Results and Analysis") attest the high quality of the sample. The specific heat of a 10.3-mg, plate-like single crystal was measured in the PPMS from 2 to 300 K in zero field. Below 50 K, measurements were also made in nine fields applied perpendicular to the *ab* plane, to a maximum $\mu_0 H = 14$ T. A different set of measurements on the same sample was reported in an earlier paper [16]. To exploit the PPMS' sensitivity to its maximum the specific heat of the addenda and the sample were measured at the same temperatures, and the platform thermometer was calibrated in each of the fields in which the specific heat was measured.

Specific-Heat Results and Analysis

The specific heat results for $H = 0$ at lower temperatures in shown in Fig. 23.1 (and shown in Fig. 1 of [4] for 2–300 K temperature range). The discontinuity in C at 36.9 K marks the transition to the superconducting state. The solid sloping lines in inset Fig. 23.1, which represent the ideally sharp mean-field transition in zero field, are the results of somewhat arbitrary, but typical, straight-line fits to the data just outside the regions of curvature associated with the broadening of the transition by sample inhomogeneity and fluctuation effects. Their extrapolations to T_c, together

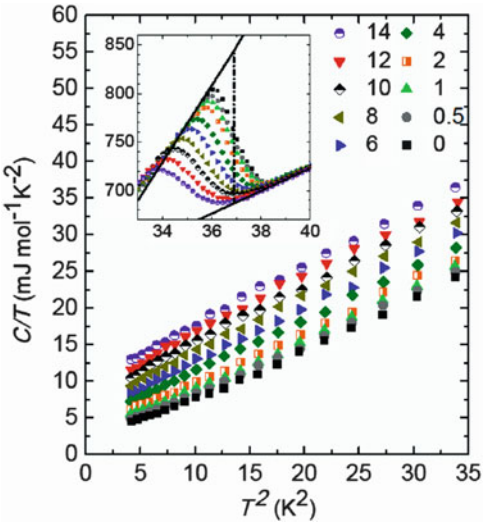

Fig. 23.1 The specific heat as C/T vs T^2 to 6 K, in 10 fields, $0 \leq \mu_0 H \leq 14$ T. The deviations from linearity suggest the presence of a low concentration of paramagnetic centers. *The inset*: The same specific heat data in the vicinity of T_c, as C/T *vs* T. The *solid sloping lines* are the results of fits to the data just outside the transition region (see text). The *dashed*, *vertical line* is an entropy-conserving construction that determines T_c as 36.9 K. The extrapolations of the solid lines to T_c represent the mean-field transition in zero field

with the entropy-conserving dash-dot vertical line, determine T_c as 36.9 K. Since $C_{lat,}$ is continuous at T_c, the solid lines give the discontinuity in C_e, $\Delta C_e(T_c)/T_c = 157.5$ mJ K^{-2} mol^{-1}. With some mathematical manipulation, $dC/dT = Td(C/T)/dT + C/T$, they also give the discontinuity in dC_e/dT, $\Delta(dC_e/dT)|_{Tc} = 1183$ mJ K^{-2} mol^{-1}. In comparison with other measurements on similar materials the transition is relatively sharp and the discontinuities are relatively large, e.g., although $\Delta C_e(T_c)/T_c$ seems to be similar to that found in one of the five measurements on similar materials (described in Sect. 6 of [4]) it is clearly larger than those in the other four.

The first step in the analysis is to obtain approximate, provisional values of γ_n and α from the data in the vicinity of T_c using α-model expressions for a single gap. The α model gives the discontinuities in C_e and dC_e/dT in terms of the parameters γ_n and α. Conversely, it can be used to obtain γ_n and α from the experimental values of the two discontinuities. For any value of α it gives C_{es} as a function of the reduced temperature, $t \equiv T/T_c$,

$$C_{es}(t)/\gamma_n T_c \equiv f_\alpha(t). \tag{23.7}$$

Since $C_{en} = \gamma_n T$, $C_{en}(T_c)/T_c = \gamma_n$, and the discontinuity in C_e at T_c is

$$\Delta C_e(T_c)/T_c = C_{es}(T_c)/T_c - C_{en}(T_c)/T_c = \gamma_n[\mathrm{f}_\alpha(1) - 1]. \tag{23.8}$$

Since $(\mathrm{d}C_{es}/\mathrm{d}t)/\gamma_n T_c = \mathrm{d}f_\alpha(t)/\mathrm{d}t \equiv \mathrm{f}_\alpha'(t) = (\mathrm{d}C_{es}/\mathrm{d}T)/\gamma_n$, and $(\mathrm{d}C_{en}/\mathrm{d}T)|_{Tc} = \gamma_n$, the discontinuity in $\mathrm{d}C_e/\mathrm{d}T$ *is*

$$\Delta(dC_e/dT)|_{Tc} = (dC_{es}/dT)|_{Tc} - (dC_{en}/dT)\big|_{Tc} = \gamma_n[\mathrm{f}_\alpha'(1) - 1]. \tag{23.9}$$

If γ_n is known independently, either Eqs. (23.8) or (23.9) would give the value of α, and each of these equations has been used in that way. However, taken together, they can be used to obtain the values of both α and γ_n: e.g., the ratios of the left- and right-hand sides of Eqs. (23.8) and (23.9) give

$$T_c\Delta(dC_e/dT)\big|_{Tc}/\Delta C_e(T_c) = [\mathrm{f}_\alpha'(1) - 1]/[\mathrm{f}_\alpha(1) - 1], \tag{23.10}$$

which determines the value of α as that for which the function of α on the right-hand side agrees with the experimental quantity on the left. With the value of α determined by Eq. (23.10), Eq. (23.8) or Eq. (23.9) can be used to obtain γ_n. The results are $\gamma_n = 32.2$ mJ K^{-2} mol^{-1}, and $\alpha = 3.27$. These would be the correct values if there were only a single band, but if there is also a small-gap band the discontinuities would have to be corrected for its contributions and the parameters of the large-gap band recalculated.

The test for the existence of a small-gap band and the determination of the characteristic parameters were based on a "global" fit with Eq. (23.5) to the data for all H and $T \leq 12$ K. It is desirable to fit the data for all H together because the H dependence of the vortex-core contribution gives important information about the energy gap (see section "Discussion") and it is best determined in a fit that takes the other contributions into account. In addition, the ratio of data points in the fit to fitting parameters is increased, reducing the uncertainties in the derived parameters (see below). The details of the final fitting expression were based on the results of trials of a number of different fitting expressions and different temperature intervals for the fits. The results of some of these preliminary fits are described, together with other evidence of the validity of the fit, in the last two paragraphs of this section. The final fitting expression made allowance for four contributions to $C(H)$: the lattice contribution, represented by three terms of Eq. (23.3); the vortex-core contribution, $\gamma_v(H)T$; the superconducting-condensate contribution, C_{es} for $H = 0$, and C_{evs} for $H \neq 0$; the paramagnetic-center contribution, represented by a two-level Schottky function (see below) with an H-dependent characteristic temperature, $\theta_{\mathrm{Sch}}(H) = \theta_{\mathrm{Sch}}(0)(1 + \beta H^2)^{1/2}$. Inclusion of the paramagnetic-center contribution was suggested by the deviations from linearity in the plot of C/T vs T^2 (see Fig. 23.1) which are typical indications of the presence of a low concentration of paramagnetic centers.

For $T \leq 12$ K the component of C_{es} associated with a large-gap band with $\alpha \sim 3$ and $\gamma_n \sim 30$ mJ K^{-2} mol^{-1} would be negligible, and it is only the component associated with a small-gap band that needs to be considered. As given by Eq. (23.7), that component would be $C_{es2}(T) = \gamma_{n2}T_c\mathrm{f}_\alpha(T)$. For this interval of

temperature and the values of α that turn out to be of interest (~1) it can be represented by the exponential of a three-term polynomial in T^{-1}, $-X_\alpha(T)$, giving

$$C_{es2}(T) = \gamma_{n2}T_c f_\alpha(T) = \gamma_{n2}T_c \exp[-X_\alpha(T)], \tag{23.11}$$

with the three coefficients in $X_\alpha(T)$ determined by the value of α. (The polynomial in T^{-1} was suggested by the T dependence of C_{es} given by the BCS theory, and it was found that sums of a constant term, a term in T^{-1}, and term in $T^{-1/2}$ gave good fits to the α-model expressions.) Generalizing that expression to extend its validity to the in-field data, i.e., to represent $C_{evs2}(H)$ for $H \neq 0$, requires allowing for its H dependence in the vortex state. There is little theoretical guidance for such a generalization, but experimental results on other superconductors suggest two changes: the replacement of the pre-exponential coefficient, $\gamma_{n2}T_c$, with an H-dependent coefficient, $a(H)$, to allow for the reduction in the magnitude of the residual superconducting condensate contribution that is complementary to the increase in the vortex core contribution, and the inclusion of an H-dependent factor, $b(H)$, in the exponent to allow for the effective reduction of the gap by the pair-breaking effect of the field. With these changes, the component of $C_{evs}(H)$ and C_{es} associated with the small-gap band is $a(H)\exp[-b(H)X_\alpha(T)]$ and the fitting expression becomes

$$C(H) = C_{lat}(T) + \gamma_v(H)T + a(H)\exp[-b(H)X_\alpha(T)] + mC_{Sch}(H,T). \tag{23.12}$$

Fitting the data for $H \neq 0$ simultaneously with the $H = 0$ data more than doubles the ratio of number of points in the fit to number of adjustable parameters, and gives more reliable values of the parameters. (However, with more precise data, which might be obtained in other apparatus, it might be possible to obtain comparably reliable values of the $H = 0$ parameters without invoking the empirical generalization of Eq. (23.11) to include the $H \neq 0$ data.)

A fit has to be made for a particular value of α, which determines the values of the three fixed parameters in $X_\alpha(T)$ that are needed to make the fit. The derived values of the adjustable parameters depend on the value of α for which the fit was made, and the correct value of α is identified by comparison of the results of fits made with different values: The third term in Eq. (23.12), with the adjustable parameters $a(H)$ and $b(H)$, represents the contribution of the superconducting condensate of the small-gap band for all H, but for $H = 0$ its T dependence is correct for the value of α for which the fit was made *only* if the derived $b(0) = 1$. This provides the criterion for recognizing the correct value of α, i.e., that for which the fit gives $b(0) = 1$. For the same reason, that fit gives γ_{n2}, as $\gamma_{n2} = a(0)/T_c$. The derived values of $b(0)$ have a strong dependence on α—e.g., $b(0) = 1.109$, 0.946, and 0.822 for $\alpha = 0.8$, 0.9, and 1.0—ensuring a precise determination of α. The result $b(0) = 1$ was obtained for $\alpha = 0.86$, and for that fit $a(0) = 337 \pm 17$ mJ K^{-1} mol^{-1}. These results show the existence of a small-gap band characterized by the parameters $\alpha_2 = 0.86$ and $\gamma_{n2} = (337 \pm 17)/36.9 = 9.1 \pm 0.5$ mJ K^{-2} mol^{-1}. Because of the small value of γ_{n2}, and particularly the small value of α_2, this

band makes only small contributions to the discontinuities at T_c: $\Delta C_{e2}(T_c)/T_c = 3.1$ mJ K^{-2} mol^{-1}; $\Delta[(dC_{e2}/dT)|_{Tc}] = 3.5$ mJ K^{-2} mol^{-1}. Correcting the measured discontinuities for these contributions gives $\Delta C_{e1}(T_c)/T_c = 154.4$ mJ K^{-2} mol^{-1} and $\Delta[(dC_{e1}/dT)|_{Tc}] = 1180$ mJ K^{-2} mol^{-1}, which in turn give $\alpha_1 = 3.30$, $\gamma_{n1} = 31.0$ mJ K^{-2} mol^{-1}, and a total $\gamma_n = 40.1$ mJ K^{-2} mol^{-1}. The characteristic parameters of the two bands are listed in Table 23.1. In Table 23.2 they are compared with the values obtained from measurements on five other near-optimally hole-doped 122 Fe-pnictide superconductors (see Sect. 6 of [4]) and the comparison suggests some consideration of the uncertainties: A quantitative measure of the uncertainty in our value of γ_{n2} is given directly by the fit, $\gamma_{n2} = 9.1 \pm 0.5$ mJ K^{-2} mol^{-1}. It is a measure of the validity of the mathematical expression for C_{es} in representing the data. The provisional value of γ_n, 32.2 mJ K^{-2} mol^{-1}, was determined from the straight-line construction in Fig. 23.1, which, in the absence of mathematical expressions for the effects of fluctuations and sample inhomogeneity on the transition, represents a qualitative estimate of those effects. The real uncertainty in γ_n arises from the way the lines were drawn. Only a qualitative estimate is possible, and, on the basis of the shape of the transition in Fig. 23.1 and comparisons with other measurements, 5% would seem to be reasonable for the uncertainty in the provisional value of γ_n and, therefore, in γ_{n1} and in the final value of γ_n, 40.1 mJ K^{-2} mol^{-1}. The more complicated analyses that led to the parameters derived from the other measurements in Table 23.2 make identification of the

Table 23.1 Characteristic parameters of the two electron bands

Electron band	α	$\Delta(0)$ (meV)	γ (mJ K^{-2} mol^{-1})
1	3.30	10.49	31.0
2	0.86	2.73	9.1

Table 23.2 Characteristic parameters of the electron bands for five other near-optimally hole-doped Fe-pnictide superconductors in the 122 series, compared with the values reported here

Composition/Reference	γ_n	α	γ_{n1}	γ_{n2}	α_1	α_2
$Ba_{0.59}K_{0.41}Fe_2As_2$/This work [4]	40.1		31.0	9.1	3.30	0.86
$Ba_{0.6}K_{0.4}Fe_2As_2$/[17, 18]	71.0	1.9				
$Ba_{0.6}K_{0.4}Fe_2As_2$/[19, 20]	9.0	2.07	9.2	39.8	3.7	1.9
$Ba_{0.68}K_{0.32}Fe_2As_2$/[21]	50.0		25.0	25.0	3.3	1.1
$Ba_{0.65}Na_{0.35}Fe_2As_2$/[22]	57.5		29.9	27.6	2.08	1.06
$Ba_{0.55}K_{0.45}Fe_{1.95}\ Co_{0.05}As_2$/[23]	40.5	2.57	34.8	5.7	3.9	0.86

The values in the top row, this work, were derived by comparing α-model expressions for the electron contribution directly with the total measured specific heat. The other values were derived in conventional analyses in which the α-model expressions were compared with a superconducting-state electron specific heat that had been obtained by subtracting an independently determined approximation for the lattice contribution from the total specific heat. The values of γ_n are the totals for two bands, however they were derived; the values of α are the results of single-band fits, if they were made; the values in the 4th–7th columns are the results of two-band fits. For the two-band fit in 19 α_1 and α_2 were fixed at values obtained from ARPES measurements. The units of γ_n, γ_{n1}, and γ_{n2} are mJ K^{-2} mol^{-1}

origins of the uncertainties and estimates of their magnitudes much more difficult, and the uncertainties are not discussed in the publications.

The other contributions to $C(H)$ obtained in the fit are plausible and consistent with the behavior shown by other superconductors, e.g., the evolution with increasing H of the different contributions in Eq. (23.12) and the derived parameters characteristic of the small-gap band, which fall within the *ranges* suggested by other measurements (see Table 23.2). The H-independent parameters obtained in the fit are: $m = 1.29 \pm 0.15 \times 10^{-3}$ mol mol^{-1}; $\theta_{Sch}(0) = 7.32 \pm 0.41$ K; $\beta = 3.30 \pm 1.17 \times 10^{-2}$ T$^{-1/2}$; $B_3 = 0.602 \pm 0.022$ mJ K^{-4} mol^{-1}; $B_5 = 7.23 \pm 2.1 \times 10^{-4}$ mJ K^{-6} mol^{-1}; $B_7 = -6.1 \pm 7.0 \times 10^{-7}$ mJ K^{-8} mol^{-1}. While the H-dependent parameters are given in a table in [4], $\gamma_v(H)$ is displayed graphically in Fig. 23.2. The evolution with increasing H of each of the three H-dependent contributions to $C(H)$ is illustrated in Fig. 23.3 for $\mu_0 H = 0$, 6, and 14 T, with the H-independent C_{lat} included for comparison. The H dependences of the coefficient of the contribution of the superconducting condensate and the energy gap that were introduced empirically, the factors $a(H)$ and $b(H)$, give a satisfactory representation of the experimental data. Furthermore, and as expected, the results of the fit are consistent with the behavior seen in measurements on other superconductors: The contribution of the superconducting condensate decreases with increasing H, as shown by the values of $a(H)$ and by the plots of C_{es2} and C_{evs2} in Fig. 23.3. The T and H dependences of C_{es2} and C_{evs2} are plausible, and the exponential downturns at low temperatures occur at temperatures consistent with

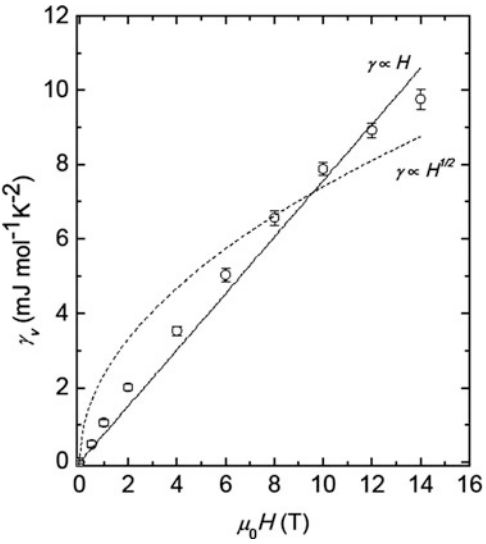

Fig. 23.2 The H dependence of $\gamma_v(H)$ as obtained in a "global" fit to the data for $2 \leq T \leq 12$ K in 10 fields, $0 \leq \mu_0 H \leq 14$ T. The *solid* and *dashed lines* represent least-squares fits to H and $H^{1/2}$ dependences. The *error bars* correspond to the uncertainties determined in the fit

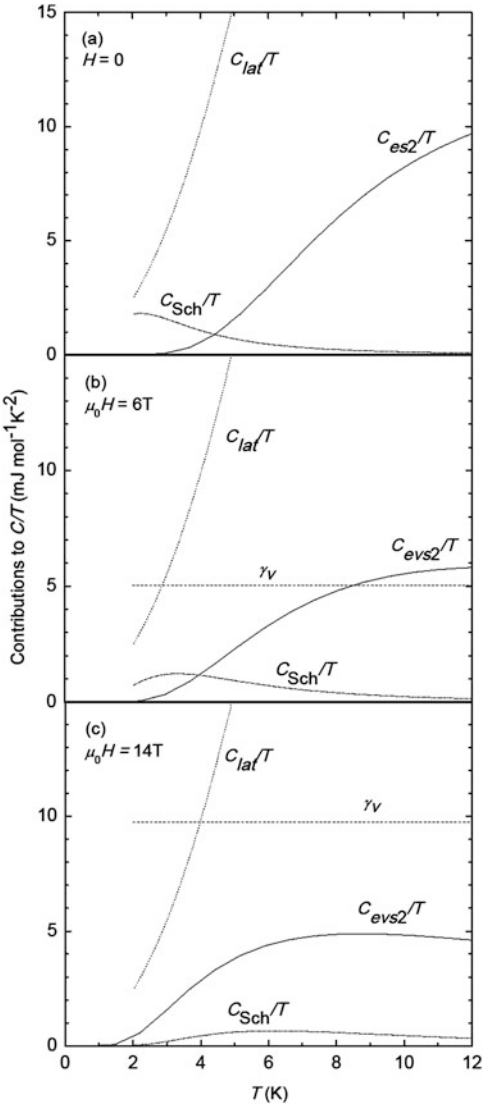

Fig. 23.3 Lattice, paramagnetic-center, and electron contributions to C/*T*, for $\mu_0 H = 0$, 6, and 14 T in (**a**), (**b**), and (**c**), as obtained in a "global" fit to the data for $2 \leq T \leq 12$ K in 10 fields, $0 \leq \mu_0 H \leq 14$ T. In (**a**) C_{es2}/T is the contribution of the small-gap band to C_{es}/T, i.e., in the superconducting state. In (**b**) and (**c**) C_{evs2}/T is the corresponding contribution of the small-gap band to C_{ev}/T, i.e., in the vortex state. In this temperature interval and on this scale the analogous contributions of the large-gap band are negligible. In (**b**) and (**c**) γ_v is the total contribution of the vortex cores

the values of $b(H)$ in showing the expected decrease in the effective gap with increasing H.

The identification of a band with a small energy gap requires the accurate determination of C_{es} at the low temperatures at which it would make a significant contribution to $C(0)$, typically $T \leq 15$ K for the small gaps that have been reported in these materials. The problem, *for any analysis*, is to identify the small C_{es2}—a maximum of only 12% of $C(0)$, near 9 K in our results—and separate it from the much greater C_{lat}. In the conventional analyses an error of only a few percent in the independently determined C_{lat} that is subtracted from $C(0)$ would have a substantial effect on any evidence for a small gap that might be obtained from the derived C_{es}. Our analysis, unlike the conventional analyses, does not require an independent, quantitative determination of C_{lat} that is subtracted from $C(0)$ before the fit is made. It does require making an *allowance* for C_{lat} in the fitting expression, and this takes the form of the sum of the $T,^3$ $T,^5$ and T^7 terms in Eq. (23.3), which is generally accepted as representing the T dependence of C_{lat} in this low-T interval. The coefficients of these three terms are an incidental byproduct of the fit, and they do determine C_{lat} in this limited T interval. However, since they were determined in the low-T fit they do not prejudice the outcome of the determination of C_{es} in the way that independently determined coefficients would. The choice of the three-term expression for C_{lat} was based on a number of preliminary fits with Eq. (23.12), eight of which, with or without the T^7 term, to either 10 or 12 K, and for α either 0.8 or 0.9, gave the same value of $a(0)$ to within $\pm 5\%$, and to within $\pm 2.5\%$ for each group of four for which α was the same. These fits suggested that the T^7 term would make only a marginal contribution, but it was included to give maximum flexibility in the determination of the other contributions. It did make only a small contribution in the final fit, and the large uncertainty in the coefficient shows that the results of the fit would have been essentially the same without it, except that a small compensating change in B_5 would be expected. The paramagnetic-center contribution presented the major problem with the fitting expression. The two-level Schottky anomaly in the final fitting expression is clearly too narrow in temperature, but broader anomalies that were tried—two-level Schottky anomalies with different degeneracies of the levels or with Gaussian or Lorentzian broadening, and a three-level Schottky anomaly—made no significant improvement in the fit and did not suggest an alternative. However, the Schottky contribution is relatively small, and significant only at the lowest temperatures and in low fields (see Fig. 23.3). Its small size accounts for the relatively large uncertainties in the parameters m, $\theta_{Sch}(0)$ and β, but it is only the sharp drop off on the high-T side, which is not sensitive to the details of the fitting expression, that is relevant to the separation of the four contributions to $C(H)$. For that reason, and because the Schottky contribution is not of any interest in itself, the inadequacy of this term in the fitting expression is not important.

In the final fitting expression, Eq. (23.12), there are 36 adjustable parameters, six of which are independent of H and represent the magnitudes and T dependences of the lattice and Schottky contributions to $C(H)$. Of the 30 H-dependent parameters, 10 represent the relatively simple H dependence expected for $\gamma_v(H)$ and 20 model

the comparably simple H dependences of the superconducting-condensate contribution, as suggested by results for other superconductors. There are 320 data points in the fit, an adequate excess over the number of parameters, especially considering the limited roles of the H-dependent parameters. The fit was made using a non-linear least-squares procedure using Matlab, and carried to the smallest convergence tolerance allowed. To ensure that the fitting process converged to the best possible result (an absolute minimum of the reduced χ^2) a number of fits were made with different initial values of the parameters and different iteration step sizes. The T dependences of the four contributions to $C(H)$ are all well defined and substantially different, which is of considerable importance in connection with the validity of their separation. While the fractional deviations in the final fit are up to $\pm 3\%$ at 2 K, where the Schottky contribution to $C(H)$ is significant, they decrease to ± 1 and $\pm 0.25\%$ at 5 and 12 K, the temperatures that define the interval that is most important for determining $C_{es2.}$ The results of the fit are generally plausible and consistent with the behavior of other superconductors. The validity of the fit is also supported by the uncertainties in the parameters, which are relatively small for the most important parameters, in particular $a(0) = 337. \pm 17.$ mJ K^{-1} mol^{-1} and $b(0) = 1.00 \pm 0.04$, which define C_{es2}. The result for C_{es2} is also supported indirectly by the strong dependence of $b(0)$ on α (see above), which is clear evidence of the existence of a term in $C(0)$ with a T dependence corresponding to the contribution of a small-gap band with a value of α within the range of the fits. The difficulties in determining C_{es2} notwithstanding, the evidence for a small-gap band characterized by $\alpha_2 = 0.86$ and $\gamma_{n2} = 9.1 \pm 0.5$ mJ K^{-2} mol^{-1} is persuasive.

Discussion

The major result of the analysis is the identification of two electron bands that contribute to the DOS, and have substantially different energy gaps in the superconducting state. [As noted in the Introduction, *some* of the measurements on other near-optimally hole-doped 122 Fe-pnictide superconductors (described in more detail in Sect. 6 of [4]) showed evidence of two gaps, and the details and references are given in Table 23.2.] The total DOS, as measured by the coefficient of the electron contribution to the specific heat, corresponds to $\gamma_n = 40.1$ mJ K^{-2} mol^{-1}, and it is comprised of a contribution, $\gamma_{n1} = 31.0$ mJ K^{-2} mol^{-1}, from the band with the larger gap, $\Delta_1(0) = 10.49$ meV, and a contribution, $\gamma_{n2} = 9.1$ mJ K^{-2} mol^{-1}, from the band with the smaller gap, $\Delta_2(0) = 2.73$ meV. The results for C_{es} and its two components are shown graphically in Fig. 23.4, with the result of the BCS theory in the weak coupling limit and for the same γ_n, included for comparison. Although circumvention of the need for an independent determination of C_{lat} is an important feature of our analysis, C_{lat}, and its relation to $C(0)$, is of some interest for comparison with the results of other measurements. The 2–12 K fit with Eq. (23.12) gives C_{lat} for that temperature interval. At higher temperatures the apparent C_{lat} can be obtained by subtracting C_{es} or C_{en} from $C(0)$, and for that

purpose the actual $C(0)$ data in the immediate vicinity of T_c were replaced by the straight lines in Fig. 23.1 that represent the idealized sharp transition. The results for C_{lat} to 40 K, the limit of the straight-line construction in Fig. 23.1, are represented by the solid lines in Fig. 23.5. The small difference between $C(0)$ and C_{lat} for $T \leq 20$ K emphasizes the sensitivity to errors in C_{lat} of a C_{es2} derived from that difference.

Several other techniques give values of the energy gaps that can be compared with those derived from the specific-heat data. Quite generally, the results obtained by these techniques suggest that there are two gaps with substantially different magnitudes in the Fe–pnictide superconductors (see, e.g., [24]). Here we focus on those obtained from angle-resolved photoemission spectroscopy (ARPES) measurements on $Ba_{1-x}K_xFe_2As_2$, which are the most extensive and detailed of the other measurements. The comparison is best made on the basis of the values of $\Delta_1(0)$ and $\Delta_2(0)$, which are given directly by the ARPES results, and are independent of T_c. In the following. $\Delta_1(0)$ and $\Delta_2(0)$ are used for the larger and smaller gaps, respectively, regardless of the notation used in the other publications. As derived from the specific-heat data, these quantities are averages in the sense that small differences between different sheets of the Fermi surface and anisotropies on a single sheet are not resolved. ARPES measurements give more detailed information but the results are often summarized by two averages over narrow ranges of gap magnitude. For a sample with $T_c = 32$ K, Evtushinsky et al. [25] report $\Delta_1(0) = 9.2 \pm 1$ meV for an inner hole-like barrel at the Γ point, and smaller gaps on all other elements of the Fermi surface. However, the feature that showed the opening of the larger gap was not observed for the smaller gaps, and they

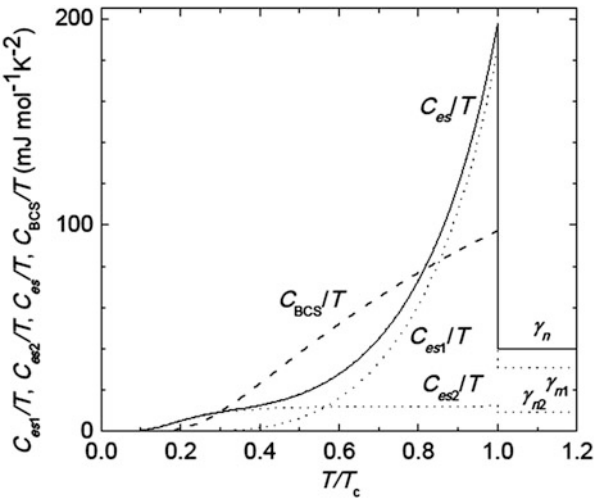

Fig. 23.4 The total electron contribution to C/T, the *solid line*, and its two components, the *two dotted lines*, as functions of T/T_c, in the superconducting state for $T/T_c \leq 1$, and in the normal state for $T/T_c \geq 1$. The large-gap component is identified by the labels C_{es1}/T and γ_{n1}, the small-gap component by the labels C_{es2}/T and γ_{n2}, and the total by the labels C_{es}/T and γ_n. The *dashed line*, C_{BCS}/T, represents the result of the BCS theory in the weak-coupling limit for the same γ_n

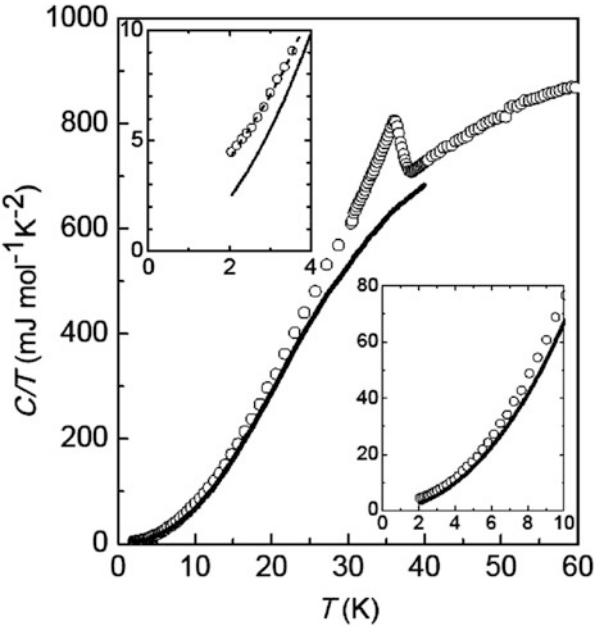

Fig. 23.5 The specific heat in zero field, as C/T *vs* T, for 2–50 K in the main panel, and for intervals at lower temperatures in the insets. The superconducting transition is marked by the sharp drop in C/T in the vicinity of $T_c = 36.9$ K. The *solid curves* represent the apparent C_{lat}, obtained by different methods, as described in the text. The *dashed curve* in the *upper inset* represents $C_{lat} + C_{\mathrm{Sch}}$ in zero field, as determined in a "global" fit to the data for $2 \leq T \leq 12$ K in 10 fields, $0 \leq \mu_0 H \leq 14$ T

conclude only that $\Delta_2(0) < 4$ meV. For a sample with $T_c = 37$ K and x = 0.4, Ding et al. [26] report $\Delta_1(0) \sim 12.5$ meV for the inner Γ barrel and $\Delta_2(0) \sim 5.5$ meV for the outer Γ barrel, but the unusual temperature dependence of the gaps leaves some doubt about the extrapolation to 0 K. For a sample with $T_c = 35$ K and x = 0.4, Zhao et al. [20] report anisotropic gaps, $\Delta_1(0) = 10$–12 ± 1.5 meV for the inner Γ barrel, and $\Delta_2(0) = 7$–8 ± 1.5 meV for the outer Γ barrel. The two Fermi surface spots near the M point are gapped below T_c but the gaps persist above T_c. For a sample with x = 0.45, but unspecified T_c, Liu et al. [27] report measurements on samples that "display bulk superconductivity" but the superconducting gaps are not detected in measurements at 12 K. Our value of $\Delta_1(0)$ falls well within the range of those obtained from ARPES results, but, while the value of $\Delta_2(0)$ is consistent with that obtained by Evtushinsky et al. [25] it is substantially lower than the other two ARPES values. Although our value was obtained from a small feature in the low-temperature specific heat, the sensitivity of the fits to the value of α_2, which determines $\Delta_2(0)$, argues against such an error in $\Delta_2(0)$. Comparably small values of $\Delta_2(0)$, as measured by α_2, have been reported in electron-doped $BaFe_2As_2$ – α_2 = 0.95 in [28] and $\alpha_2 = 0.957$ in [29]—but, given the differences between the

electron- and hole-doped compounds, the implications of this similarity in the values of α_2 are not clear.

The H dependence of $\gamma_v(H)$ gives information about the symmetry of the order parameter, most directly on the existence of nodes. For "conventional" s-wave superconductors with an isotropic gap, $\gamma_v(H)$ varies linearly with H. For a d-wave superconductor Volovik predicted an $H^{1/2}$ dependence associated with extended quasiparticle states near line nodes [30]. This effect was first observed by Moler et al. [31] in a cuprate superconductor. It has been suggested that this $H^{1/2}$ dependence is modified to $H\ln H$ at low fields in a dirty superconductor [32]. Modifications of the H-proportional dependence in the case of an isotropic gap, negative curvature in high fields, have also been suggested [33]. The H dependence of $\gamma_v(H)$ is compared with H and $H^{1/2}$ dependences in Fig. 23.2. Overall, $\gamma_v(H)$ is better represented by the solid straight line, which has a slope 0.75 mJ K^{-2} mol^{-1} T^{-1}, than the dashed curve for $H^{1/2}$. (The $H\ln H$ dependence suggested for a dirty d-wave superconductor [32] would not give a better fit.) For this reason, and particularly because the low-field data suggest a finite limiting slope, these results are more consistent with an isotropic gap than with the low-energy excitations associated with nodes. Two other measurements of $\gamma_v(H)$, to 9 T, on K-doped $BaFe_2As_2$ have been interpreted in the same way: For $Ba_{0.6}K_{0.4}Fe_2As_2$ an approximately H-proportional dependence [17] with a slope 0.63 mJ K^{-2} mol^{-1} T^{-1}, and for $Ba_{0.55}K_{x0.45}Fe_2As_2$ a more precisely determined H-proportional dependence [23] with a slope 0.60 mJ K^{-2} mol^{-1} T^{-1} have been reported. There is no obvious explanation for the curvature in $\gamma_v(H)$ in Fig. 23.2. The curvature predicted for an isotropic gap [33] seems to be significant only at higher fields. For MgB_2 there is a relatively sharp bend in $\gamma_v(H)$ vs H that is associated with different values of H_{c2} for the two bands [34], and perhaps an effect of that kind, but with a smaller difference in the values of H_{c2}, could be at work here. It is also interesting that a calculation of the "Volovik" effect for a two-band superconductor with different isotropic gaps and impurity scattering [35] gives a transition from the generic H-proportional dependence of $\gamma_v(H)$ at low H to something approaching $H^{1/2}$ at higher H. The resulting negative curvature of $\gamma_v(H)$ depends on the ratio of the gap sizes and is particularly strong for ratios of the order of 3.3 to 5. However, the calculations give substantial non-zero values of $\gamma_v(0)$, precluding quantitative comparison with our results.

Band-structure calculations [36] for $Ba_{1-x}K_xFe_2As_2$ using the local-density approximation (LDA), the virtual-crystal model, and allowing the positions of the As atoms to relax according to the LDA energy minimization criterion, show a very weak dependence of the DOS on doping. For the undoped $BaFe_2As_2$ the "bare" band-structure DOS is $N(E_F) = 3.06$ states eV^{-1} $f.u.^{-1}$; for the $x = 0.4$ hole-doped material $N(E_F) \sim 3.12$ states eV^{-1} $f.u.^{-1}$. However, the rigid-band calculation [36] which gave essentially the same result for $x = 0$, gave $N(E_F) \sim 4.38$ states eV^{-1} $f.u.^{-1}$ for $x = 0.4$ [36]. Another calculation [37] gave $N(E_F) = 4.553$ states eV^{-1} $f.u.^{-1}$ for $BaFe_2As_2$, and, using a supercell model, $N(E_F) = 5.526$ states eV^{-1} $f.u.^{-1}$ for $x = 0.5$. The increase in $N(E_F)$ for $x = 0.5$ in that calculation was ascribed to the use of the fixed experimental As position for the undoped compound [36]. For

comparison with experimental quantities, we take, somewhat arbitrarily, the value $N(E_F) = 3.12$ states eV^{-1} f.u.$^{-1}$ from [36]. The corresponding electron contribution to the specific heat, represented as the coefficient of a T-proportional term, is $\gamma_0 = 7.35$ mJ K^{-2} mol^{-1}. The experimental value of γ_n, 40.1 mJ K^{-2} mol^{-1}, then suggests an effective mass renormalization that would be unusually strong for a simple metal, for which the mass renormalization is produced by the electron-phonon interaction represented by the electron-phonon coupling parameter (λ) and $\gamma_n = (1 + \lambda)\gamma_0$. The value of λ would be 4.5, a factor 10 or so higher than the values commonly attributed to the electron-phonon interaction in "simple" metals. The theoretical value of $N(E_F)$ chosen for the comparison was among the lowest, but the experimental value of γ_n was also among the lowest (see Sect. 6 of [4]), and any of the possible comparisons would still give an extraordinarily high value of λ. Although the mass renormalization for F-doped LaOFeAs, in the 1111 series of Fe pnictide superconductors is not as strong as that found here for a member of the 122 series, it is strong enough to have attracted attention and it has motivated several calculations of the electron-phonon interaction. In one calculation [38], the electron-phonon λ was found to be ~0.2, and in another [39] 0.21. In both cases it was concluded that these numbers are too small to explain the apparent mass renormalization, and that the electron-phonon interaction is also too weak to account for the observed T_c. There are differences between the 1111 and 122 series, but, since the superconductivity occurs in the FeAs layers in both, it is reasonable to assume that these conclusions, with some allowance for differences in the numbers, would apply to $Ba_{1-x}K_xFe_2As_2$. It therefore seems likely that calculation of the electron-phonon interaction for $Ba_{0.59}K_{0.41}Fe_2As_2$ would not account for the observed mass enhancement.

The electron-phonon interaction accounts for both the normal-state mass renormalization and the superconducting-state electron pairing in "conventional" superconductors. The fact that it doesn't account for either in the Fe pnictides raises the question as to whether there is another interaction that contributes to both. Interaction with spin fluctuations, which can support spin-singlet superconductivity only if there is a sign-changing order parameter, has been suggested as the mechanism for the electron pairing [38]. It was also suggested that the pairing would be "extended" s wave, designated $s_{\pm}$, in which isotropic order parameters on different sheets of the Fermi surface have opposite signs [38]. The approximate linearity of $\gamma_v(H)$ in H (see Fig. 23.2) supports the argument in [38] that the $s_{\pm}$ pairing is more likely than d-wave, which could also satisfy the requirement of a sign-changing order parameter, but which would have nodes in the energy gaps. With respect to the mass renormalization, it is suggested in [40], which includes a general comparison of the superconductivity in the 1111 and 122 series, that while spin fluctuations might produce the strong mass enhancement in the 1111 series they might not produce the stronger effect in the 122 series. However, there seem to be no quantitative calculations. The specific-heat results emphasize the importance of theoretical consideration of magnetically mediated electron-electron interactions and their role in both mass enhancement and the occurrence of superconductivity. In connection with other theoretical predictions, we note that, in common with most

other experimental work, the relations between energy gaps and the DOS that we report seem to be inconsistent with a theory of the superconductivity [40] based solely on interband interactions.

Summary

The specific heat of a high-quality single crystal of $Ba_{0.59}K_{0.41}Fe_2As_2$, a near-optimally hole-doped superconductor in the 122 series of Fe pnictides, was measured from 2 to 300 K, and below 50 K in fields to $\mu_0 H = 14$ T.

A novel method of analysis of the data, based on *direct* comparisons of α-model expressions for the *electron contribution* with the *measured total specific heat*, was used to obtain the parameters characteristic of the electron bands. It bypasses the independent determination of the lattice contribution, an essential step in the conventional analyses, in which the lattice contribution is subtracted from the total to obtain the electron contribution, and it eliminates the substantial uncertainties in the electron contribution associated with the approximations inherent in the determination of the lattice contribution. The derived parameters characteristic of the electron contribution are significantly different from those obtained by conventional analyses for a group of five other near-optimally hole-doped $BaFe_2As_2$ superconductors, which also show significant differences within the group. We suggest that the approximations used in obtaining the lattice contribution in the conventional analyses make an important contribution to these differences.

For $Ba_{0.59}K_{0.41}Fe_2As_2$ the total DOS, as measured by the value of γ_n, 40.1 mJ K^{-2} mol^{-1}, is the sum of two contributions, $\gamma_{n1} = 31.0$ mJ K^{-2} mol^{-1} and $\gamma_{n2} = 9.1$ mJ K^{-2} mol^{-1}, from bands with superconducting-state energy gaps that are, respectively, larger and smaller than the weak-coupling BCS value. As measured by the gap-proportional parameter α, which is $1.764 \equiv \alpha_{BCS}$ in the weak-coupling limit of the BCS theory, the gaps correspond to $\alpha_1 = 3.30$ and $\alpha_2 = 0.86$. The energy gaps derived from the specific-heat data are within the ranges of values obtained in ARPES measurements, but there are some significant differences. The H dependence of the T-proportional term in the vortex-state specific heat suggests a nodeless order parameter and is consistent with extended s-wave pairing. The relations between the DOS and energy gaps for the two bands are not consistent with theoretical predictions [41] for a model in which superconductivity is produced by interband interactions alone. Comparison of the total DOS, as deduced from the value of γ_n, with band-structure calculations shows a strong effective mass renormalization that is without precedent in simple metals and is not theoretically explained.

Acknowledgements This work was supported by the Director, Office of Science, Office of Basic Energy Sciences, U.S. Department of Energy, under Contract No. DE-AC02-05CH11231 and Office of Basic Energy Sciences U.S. DOE under Grant No. DE-AC03-76SF008. We are grateful

to J. E. Gordon for help with the α-model calculations and helpful discussions about the method of analyzing the data.

References

1. J. G. Bednorz, K. A. Müller, Z. Physik B Condens. Matt. **64**, 189 (1996)
2. J. Nagamatsu, N. Nakagawa, T. Muranaka, Y. Zenitani, J. Akimitsu, Nature **410**, 63 (2001)
3. Y. Kamihara, T. Watanabe, M. Hirano, H. Hosono, J. Am. Chem. Soc. **130**, 3296 (2008)
4. C.R. Rotundu, T.R. Forrest, N.E. Phillips, R.J. Birgeneau, JPSJ **84**, 114701 (2015)
5. B. Mühlschlegel, Z. Phys. **155**, 313 (1959)
6. H. Padamsee, J.E. Neighbor, C.A. Shiffman, J. Low Temp. Phys. **12**, 387 (1973)
7. F. Bouquet, Y. Wang, R.A. Fisher, D.G. Hinks, J.D. Jorgensen, A. Junod, N.E. Phillips, Europhys. Lett. **56**, 856 (2001)
8. H.J. Choi, D. Roundy, H. Sun, M.L. Cohen, S.G. Louie, Nature (London) **418**, 758 (2002)
9. C. Caroli, P.G. de Gennes, J. Matricon, Phys. Lett. **9**, 307 (1964)
10. N.W. Ashcroft, N.D. Mermin, *Solid State Physics* (Saunders College, Philadelphia, 1976)
11. J.G. Storey, J.W. Loram, J.R. Cooper, Z. Bukowski, J. Karpinski, arXiv:1001.0474v1
12. G. Grimvall, J. Phys. Chem. Solids **29**, 1221 (1968)
13. P.B. Allen, M.L. Cohen, Phys. Rev. B **1**, 1329 (1970)
14. J.J. Sabo Jr., Phys. Rev. B **1**, 1325 (1970)
15. H. Luo, Z. Wang, H. Yang, P. Cheng, X. Zhu, H.-H. Wen, Supercond. Sci. Technol. **21**, 125014 (2008)
16. C.R. Rotundu, B. Freelon, S.D. Wilson, G. Pinuellas, A. Kim, E. Bourret-Courchesne, N.E. Phillips, R.J. Birgeneau, J. Phys. Conf. Ser. **273**, 012103 (2011)
17. U. Welp, G. Mu, R. Xie, A.E. Koshelev, W.K. Kwok, H.Q. Luo, Z.S. Wang, P. Cheng, L. Fang, C. Ren, H.-H. Wen, Phys. C **469**, 575 (2009)
18. G. Mu, H. Luo, Z. Wang, L. Shan, C. Ren, H.-H. Wen, Phys. Rev. B **79**, 174501 (2009)
19. C. Kant, J. Deisenhofer, A. Günther, F. Schrettle, A. Loidl, M. Rotter, D. Johrendt, Phys. Rev. B **81**, 014529 (2010)
20. L. Zhao, H.-Y. Liu, W.-T. Zhang, J.-Q. Meng, X.-W. Jia, G.-D. Liu, X.-L. Dong, G.-F. Chen, J.-L. Luo, N.-L. Wang, W. Lu, G.-L. Wang, Y. Zhou, Y. Zhu, X.-Y. Wang, Z.-Y. Xu, C.-T. Chen, X.-J. Zhou, Chin. Phys. Lett. **25**, 4402 (2008)
21. P. Popovich, A.V. Boris, O.V. Dolgov, A.A. Golubov, D.L. Sun, C.T. Lin, R.K. Kremer, B. Keimer, Phys. Rev. Lett. **105**, 027003 (2010)
22. A.K. Pramanik, M. Abdel-Hafiez, S. Aswartham, A.U.B. Wolter, S. Wurmehl, V. Kataev, B. Büchner, arXiv:1106.5471v1
23. K. Gofryk, J.C. Lashley, F. Ronning, D.J. Safarik, F. Weickert, J.L. Smith, A. Leithe-Jasper, W. Schnelle, M. Nicklas, H. Rosner, Phys. Rev. B **85**, 224504 (2012)
24. D.V. Evtushinsky, D.S. Inosov, V.B. Zabolotnyy, M.S. Viazovska, R. Khasanoc, A. Amato, H.-H. Klauss, H. Luetkens, C. Niedermayer, G.L. Sun, V. Hinkov, C.T. Lin, A. Varykhalov, A. Koitzsch, M. Knupfer, B. Büchner, A.A. Kordyuk, S.V. Borisenko, New J. Phys. **11**, 055069 (2009)
25. D.V. Evtushinsky, D.S. Inosov, V.B. Zabolotnyy, A. Koitzsch, M. Knupfer, B. Büchner, M.S. Viazovska, G.L. Sun, V. Hinkov, A.V. Boris, C.T. Lin, B. Keimer, A. Varykhalov, A.A. Kordyuk, S.V. Borisenko, Phys. Rev. B **79**, 054517 (2009)
26. H. Ding, P. Richard, K. Nakayama, K. Sugawara, T. Arakane, Y. Sekiba, A. Takayama, S. Souma, T. Sato, T. Takahashi, Z. Wang, X. Dai, Z. Fang, G.F. Chen, J.L. Luo, N.L. Wang, Europhys. Lett. **83**, 47001 (2008)

27. C. Liu, G.D. Samolyuk, Y. Lee, N. Ni, T. Kondo, A.F. Santander-Syro, S.L. Bud'ko, J.L. McChesney, E. Rotenberg, T. Valla, A.V. Fedorov, P.C. Canfield, B.N. Harmon, A. Kaminski, Phys. Rev. Lett. **101**, 177005 (2008)
28. F. Hardy, T. Wolf, R.A. Fisher, R. Eder, P. Schweiss, P. Adelmann, H.V. Löhneysen, and C. Meingast, Phys. Rev. B **81**, 060501(R) (2010)
29. K. Gofryk, A.S. Sefat, E.D. Bauer, M.A. McGuire, B.C. Sales, D. Mandrus, J.D. Thompson, F. Ronning, New J. Phys. **12**, 023006 (2010)
30. G.E. Volovik, JETP Lett. **58**, 469 (1993)
31. K.A. Moler, D.J. Baar, J.S. Urbach, R. Liang, W.N. Hardy, A. Kapitulnik, Phys. Rev. Lett. **73**, 2744 (1994)
32. C. Kübert, P.J. Hirschfeld, Solid State Commun. **105**, 459 (1998)
33. N. Nakai, P. Miranovic, M. Ichioka, K. Machida, Phys. Rev. B **70**, 100503 (2004)
34. F. Bouquet, Y. Wang, I. Sheikin, T. Plackowski, A. Junod, S. Lee, S. Tajima, Phys. Rev. Lett. **89**, 257001–257001 (2002)
35. Y. Bang, Phys. Rev. Lett. **104**, 217001–217001 (2010)
36. D.J. Singh, Phys. Rev. B **78**, 094511 (2008)
37. I. R. Shein and A. L. Ivanovskii, arXiv: 0806.0750 (unpublished)
38. I.I. Mazin, D.J. Singh, M.D. Johannes, M.H. Du, Phys. Rev. Lett. **101**, 057003 (2008)
39. L. Boeri, O.V. Dolgov, A.A. Golubov, Phys. C **469**, 628 (2009)
40. O. V. Dolgov, I. I. Mazin, D. Parker, and A. A. Golubov, Phys. Rev. B **79**, 060502(R) (2009).
41. I.I. Mazin, J. Schmalian, Phys. C **469**, 614 (2009)